Article

Smart Wireless Climate Sensor Node for Indoor Comfort Quality Monitoring Application

C. Bambang Dwi Kuncoro [1,*], Arvanida Feizal Permana [1], Moch Bilal Zaenal Asyikin [1] and Cornelia Adristi [2]

[1] Department of Refrigeration, Air Conditioning and Energy Engineering, National Chin-Yi University of Technology, Taichung 41170, Taiwan; arvanida.permana@gmail.com (A.F.P.); bilalmoch@gmail.com (M.B.Z.A.)

[2] Department of Electrical Engineering, Faculty of Engineering, Universitas Indonesia, Depok 16424, Indonesia; cornelia.adristi@gmail.com

[*] Correspondence: bkuncoro@ncut.edu.tw; Tel.: +886-4-239-24505 (ext. 8274)

Abstract: The indoor environment climate should be controlled by continuously maintaining the temperature and relative humidity to achieve thermal comfort. A monitoring system of both parameters is the first step to improving indoor comfort quality. This paper presents a smart wireless climate sensor node for indoor temperature and humidity monitoring with a powering strategy and design approach for autonomous operation. The data logging results are sent to the cloud using Internet of Things protocol for thermal comfort monitoring and analysis. The monitoring and analysis results are useful to monitor and control the indoor thermal comfort condition for room occupants. A sensor node was designed that includes a low-power mode and compact size features. It consists of a built-in AVR-based microcontroller, a temperature and humidity sensor, and a wireless module with a supercapacitor as the power storage. A low-power algorithm and Internet of Things system were implemented to reduce the total energy consumption as low as possible during operation while improving the thermal comfort quality. This developed sensor node has a small error for temperature, and relative humidity sensed values resulting from calibration. At the same time, it also consumes low power for one cycle of data acquisition. The device was integrated with an Internet of Things monitoring system to monitor indoor thermal comfort in the field experiment. The experiment results showed that the indoor temperature and relative humidity were measured and recorded in the range of 25–30 °C and 30–40%, respectively. This prototype is a preliminary design to achieve an autonomous sensor node with a low-power energy consumption goal. Thus, with this feature, the developed sensor node has potential to couple with a micro energy harvester module toward a fully autonomous active node in further development.

Keywords: indoor air quality; autonomous sensor node; indoor comfort; Internet of Things

1. Introduction

Several factors influence indoor environmental quality (IEQ) and occupant comfort. The current indoor environmental evaluation, also known as indoor air quality (IAQ) and thermal comfort (TC), are the two components required for occupant comfort [1]. The TC environment provides a relatively low temperature for the internal building area and does not consume much energy. Therefore, Zeiler et al. present that building energy consumption has become more reasonable and controllable, and operations now account for almost 40% of worldwide energy usage [2]. With the growing electricity bills and limited operational budgets, it is becoming more crucial than ever for homeowners and companies to save money on energy. The most important aspect of any energy optimization is a thorough understanding of how a structure and its components utilize and waste energy. Nilsson et al. also explain that the built environment's energy usage is dominated by office buildings, which account for 40% of the total consumption. For general civil or commercial construction, various appliances account for a large amount of the energy

budget (up to 50%) [3]. The air conditioning system provides ventilation and heating and has become the most energy-intensive appliance for households and buildings, as shown in Table 1. In general, power consumption is determined by the frequency with which the devices are used. According to Table 1, electronic appliances, air conditioners, irons, rice cookers, washing machines, and water heaters are required to be used at different times throughout the day.

Table 1. Common appliances used in civil building [4].

Appliances	Measured Power (kW)	Energy Usage from Monday to Friday (kWh/day)	Energy Usage from Saturday to Sunday (kWh/day)
Air conditioner	1.2	6.06	9.69
Electric kettle	2–2.2	1.056	0.968
Water heater	2	0.32	3
Hairdryer	1.2	0.12	0.06
Electric Iron	1.4	0.742	0.644
Washing machine	0.85	0.884	0.884
Microwave	1–1.1	0.198	0.187

Buildings with improved insulated walls, airtight construction, and high-efficiency windows significantly influence the internal climate [5]. As seen by the increased dedication to zero-energy buildings [6], the value of buildings in promoting energy conservation is becoming more generally recognized. In Central Europe [7], studies about passive house and zero-energy building standards aim to reduce the object's thermal loss to the point where the heating system uses the least amount of energy possible. The measurement for the quantity of energy used for heating should not exceed 15 kWh/m^2, and the total primary energy demand for the object should not exceed 120 kWh/m^2. As another method, renovating an outdated air conditioner (AC) is one approach to drastically reduce building energy use. Furthermore, maintaining the use and time operation of this device necessitates a constant monitoring system of the indoor temperature and how the occupants feel comfortable to minimize its energy consumption.

In today's building automation, achieving the standard comfort quality for the indoor environment requires a more complex real-time comfort measurement. Some studies regarding thermal comfort were conducted to monitor the indoor thermal environment. Berardi et al. built a monitoring system that manually adjusts the parameters such as temperature, luminosity, and relative humidity for energy saving [8]. The results revealed various orientations and internal gains were taken to reduce the overlapping energy of using latent thermal energy system storage capacity in indoor buildings in Canada. Silveira et al. developed a wireless sensor network using 802.15.4/802.11 gateway to sense the temperature within a building [9]. This study demonstrated that the wireless sensor network signal quality and maximum communication range were tested as well as the sensor node battery lifespan predictions. In ref. [10], a sensor node system based on IEEE 1451 standard was applied in smart comfort sensing to provide energy efficiency; hence, monitoring becomes more viable for green buildings. The sensor's accuracy was calibrated and guaranteed with the used standard, and accurate measurement results were achieved after the signal processing circuit. A smartphone android-based sensing system for temperature and humidity monitoring was introduced in [11]. The user can communicate with the sensing device through a smartphone. Furthermore, 24 h battery testing revealed that it used less than 0.54 watts to operate, attaining the low-cost goal. Another study developed occupant-behavior-based thermal comfort to obtain the data and adjust the thermal comfort for the building [12]. In this case, the occupant utilized radiant-based HVAC for thermal comfort quality, and dedicated indoor air systems for air quality were

frequently found in building surveys where satisfaction with IEQ is high. Darji et al. improved temperature and humidity monitoring using Internet of Things (IoT)-based sensors with cloud data storage [13]. This sensor is cost-effective and offers automatic humidity with temperature reading and control. It also sends data to a secure server to monitor or control the system's temperature and humidity. Scislo et al. introduced repeated measurements at variable temperatures in the Variable Air Volume (VAV) and the gateway usage to determine the average measured values of the sensors, thereby preprocessing the raw data. If the measuring system is activated (for example, when the temperature reaches a specific level or an occupant enters the apartment), the gateway's algorithm can recognize such occurrences and begin recording and transferring data [14]. The parameters to quantify comfort quality, such as the level of clothing, activities, and mean radiant temperature from ISO7730 standards, was considered in the study [15]. In ref. [16], a sensor unit system was designed as a standalone wireless sensor to sense temperature and humidity. Their data can be sent over a low-energy Bluetooth transmitter and be received by the receiver node. The recorded data can be seen using portable monitoring devices, such as a Personal Computer. The importance of the indoor effect of the temperature is introduced in ref. [17]. The supply air temperature on thermal comfort in a room or ceiling heating and mixing or displacement ventilation was also presented. When the supply air temperature ranges from 15 °C to 19 °C, the ventilation distribution, velocity, as well as global temperature in the occupied zone were measured. The results can be used to recommend the use of a hybrid system (radiant heating and mechanical ventilation system) for residential and commercial buildings.

The capability of the sensor node and thermal comfort monitoring method was improved over time as presented in some studies above. However, the development of the sensor nodes for indoor thermal comfort monitoring should consider its power consumption aspect and compact design in a single board system. The goals are to achieve long-time operation with a built-in power source system to work autonomously and be easily set up within infinite space for indoor monitoring applications.

This paper introduces the development of a sensor node that can monitor indoor air quality data such as temperature and humidity and send the data logging results using an IoT protocol to the cloud for thermal comfort monitoring and analysis purposes. The sensor node includes a low-power mode and compact size features. The developed device is a preliminary design with a semi-autonomous feature that utilizes built-in rechargeable power storage as the main power source. It was designed with a low-power system mode feature to reduce the energy consumption, compact design, and utilized with an IoT system for real-time and continuous indoor climate as well as thermal comfort monitoring applications. The usage of IoT systems to store the sensing data also reduces overall system power consumption that cannot be achieved if the developed sensor node uses a commercial data logger. Moreover, the user can access the monitoring data everywhere and anytime. Considering the features above, the developed sensor node will be possible to integrate with a micro energy harvester. The harvester module can harvest energy sources from the indoor environment (light from the lamp, heat from devices, airflow from AC or electric fan, etc.) and become the power source for the autonomous sensor node in further development.

2. Materials and Methods

2.1. Indoor Comfort Quality

In the contribution to indoor environmental quality, the IAQ and the indoor comfort quality (ICQ) are two unique and distinct problems. For example, the monthly mean air temperatures are occasionally used to determine thermal comfort for indoor conditions [16]. The American Society of Heating, Refrigeration, and Air Conditioning Engineers [18] provides industry rules for building professionals. In low-rise residential and high-rise structures, indoor air quality is covered by ANSI/ASHRAE Standard 62.2 and 62.1, respectively, while thermal settings by ANSI/ASHRAE Standard 55 Thermal Environmental

Conditions for Human Occupancy. When it comes to defining conditions for thermal comfort, there are six major considerations. In some cases, comfort is influenced by several additional secondary elements. The six main components are metabolic rate, air temperature, airspeed, clothing insulation, radiant temperature, and humidity [19–21]. Another study reveals that thermal comfort is influenced by both environmental factors and human personal characteristics (age, gender, etc.) [22]. Room occupants with different genders felt different thermal sensation scales that varied in temperature, as presented in Figure 1. Thus, every room's occupant may have a different thermal comfort zone. One person may not be as able to sense the same temperature as the other person even if they are in the same room at the same time. Therefore, people entering a room that fulfills the requirements of comfort standard (ASHRAE Standard) may not find the surroundings instantly pleasant when they were recently exposed to various environmental conditions. For about an hour, the effect of earlier exposure or activity may affect comfort perceptions.
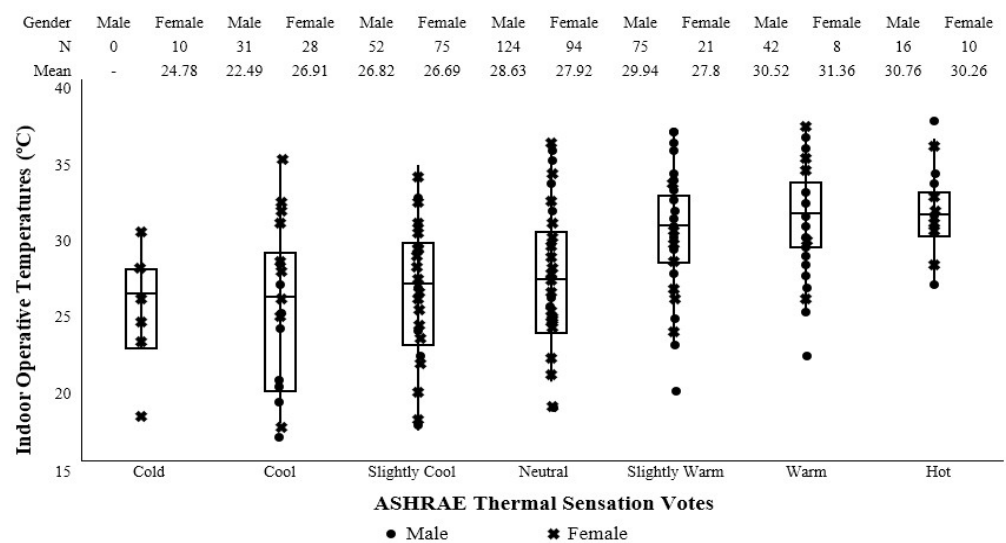
Figure 1. Boxplots and dot plots of the seven-point thermal sensation scale ASHRAE, with a statistical summary of indoor air temperatures (°C) related to ASHRAE votes filtered by gender on the top. Adapted from ref. [22]. 2020, the authors.

2.2. Temperature Standard

The surroundings and any human activities that occur inside the room are sources of the temperature that can be monitored indoors. The human temperature regulating system allows physiological adaptation to thermal stress and physical thermal comfort in several settings. Since humans are complex organisms, they maintain a constant and warm body temperature relatively to and independent from the ambient temperature, resulting in a core body temperature average of around 37 °C. The human body and the surrounding environment exchange heat by transferring it from a warm to a colder object until equilibrium is reached. This transfer condition involves two systems, with the temperature difference between them facilitating the transmission. The standard effective temperature is an equation of derivation between two nodes of the temperature from the human body control model of Gagge in 1971 [23]. Table 2 shows a standard effect of the body temperature. Ref. [24] described a body model divided into two layers, namely the core and the skin. As the metabolism generates a heat source in the core layer, the other heat is directly lost to the environment through breathing, while the rest is transferred to the skin's surface and partially lost through sweat evaporation. The remainder is sent to the clothing's surface and evaporates through radiation to the environment.

Table 2. Standard effective temperature. Adapted from ref. [23]. 2015, the authors.

SET/°C	Thermal Feeling Level	Discomfort Level	Temperature Regulation of Human Body	State of Health
40	Very hot	Intolerable	Water cannot be evaporated from the skin	Heatstroke increased risk
35–40	Hot	Very uncomfortable		
35		Uncomfortable		
30–35	Warm	A bit uncomfortable	Expanding of blood vessels and sweating	
30				
25–30	A bit warm			
25			None showed sweating	
20–25	Neutral	Comfortable		Normal state
20	A bit cool		Retraction of blood vessel	
15–20	A bit cold	A bit uncomfortable		
15			Change behaviors	
10–15	Cold		Start chilling	Body metabolism is weakened
10	Very cold	Uncomfortable		

2.3. Indoor Humidity Standard

Indoor humidity can be measured and controlled by mechanical systems. It is a matter of system selection, equipment sizing, and humidity control to meet the standard's recommendation of keeping indoor humidity between 30% and 60% RH. To manage space, traditional constant-volume systems rely on coincidental dehumidification. With today's systems, it is possible to "actively" control this parameter. The load profile of the building and the HVAC system's psychrometric performance are analyzed under all operating situations to ensure that the performance parameters are satisfied. As for relative humidity still closely related with the dry bulb temperature, Table 3 shows the classification of the indoor comfort equivalent temperature and humidity for each percentage that varies from 30% to 80% RH, and also indicates the comfort range between two different seasons of winter and summer.

Lower relative humidity levels are linked to mucous membranes and skin drying, which subsequently increases skin pain, resulting in feelings of irritation and chapping. Static electricity is created by low relative humidity, which is unpleasant and can cause computers and paper processing equipment to malfunction. Condensation within the building structure and on interior or external surfaces as well as the following development of molds and fungi can be caused by high humidity levels. The optimum zone as described in Figure 2 ranges from 30–60% RH; however, some of the health aspects might still widely occur at the zone.
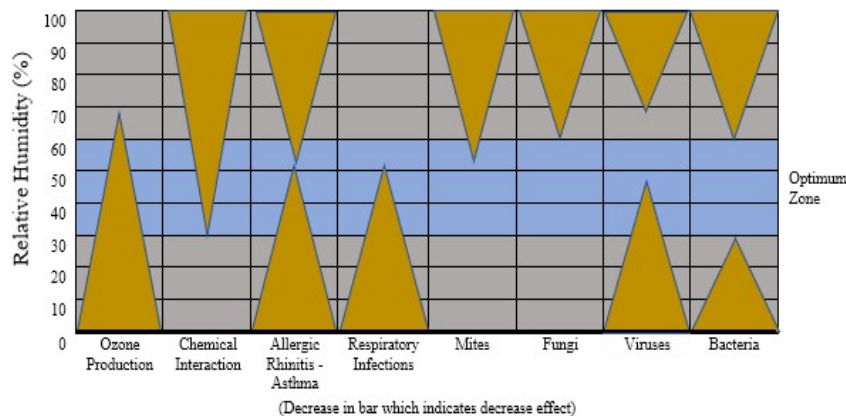
Figure 2. Humidity comfort level from a health aspect [26].

Table 3. Indoor comfort equivalent temperature and humidity level. Adapted from ref. [25].

Room Dry Bulb Temperature (°F)	Equivalent Temperature (°F)					
	RH 80%	RH 70%	RH 60%	RH 50%	RH 40%	RH 30%
62	66	65	64.5	64	63	62
63	67	66	65.5	65	64	63
64	67.5	67	66	65.5	65	64
65	69	68	67.5	67	66	65
65	70	69	68	67.5	66.5	66
66	71	70	69	68	67.5	66.5
68	72	71	70	69.5	68.5	67.5
68	73	72	71	70	69	68
69	73.5	72.5	71.5	70.5	70	69
69	74.5	73.5	72.5	71.5	70.5	69.5
70	76	75	74	73	71.5	70.5
71	77.5	76	75	74	73	71.5
72	78	77	76	75	73.5	72
73	79	78	77	75.5	74	73
74	80	79	78	76	75	74
75	81	79.5	79	77	76	75
76	82.5	80	79.5	78	77	76
77	83	81.5	80	79	78	77
78	84	83	81.5	80	79	78
79	85	84	83	81.5	80	79
80	86	85	84	83	81.5	80

Light grey: Winter comfort range
Dark grey: Summer comfort range

2.4. Continuous Indoor Comfort Monitoring

As indoor comfort mostly needs to be monitored continuously, the system's design should be considered in several aspects, such as the durability, reliability, and adaptability to be placed in various environments. Therefore, the hardware design, especially the sensor, should be a fully compact system but also flexible enough to adapt. This sensor is regarded to have a big scale and can obtain a sampling time as quickly as possible to detect air quality. Furthermore, the indoor comfort value can be readily maintained.

One architecture example for the above monitoring system was introduced in ref. [27]. The design of a monitoring method was presented with a low-cost feature that enables continuous monitoring of polluting gas concentrations in different parts of a city. In this study, the system is limited to an outside air quality monitor, with individual sensor boards installed at each location to provide data measurements directly to a centralized server through the Internet. The node is based on a Libelium embedded solution. For database management, PostgreSQL is utilized, and the sensor visualization using GMaps Application Programming Interfaces (APIs), Apache webserver, and graph visualization using Javascript library. Sensor devices continuously monitor vibration, temperature, humidity, light, and the electrical load of the air conditioning system. The provided system aims to present an accurate analysis of how IAQ sensor nodes work for monitoring indoor conditions, inhabitant comfort level recognition, automatic forecasting, as well as recommendations on the best balance between environmental quality and power needs. The IAQ architecture as described above is shown in Figure 3.
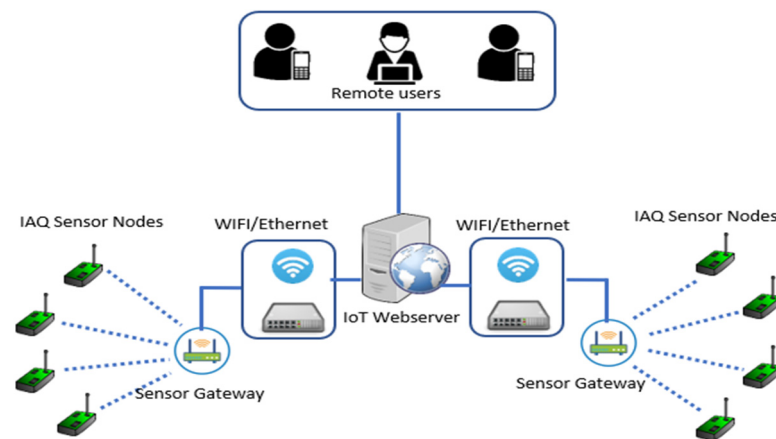
Figure 3. IAQ monitoring from various locations. Adapted from ref. [28]. 2018, the authors.

2.5. Design Overview

In this study, a smart, wireless, low-power, and autonomous sensor node was applied in an indoor climate environment monitoring application. The overall proposed sensor node comprises four main units: sensor, processor, energy storage, and transceiver. Its entire units are connected by the power distribution (orange line) and the data distribution (blue line), as shown in Figure 4.
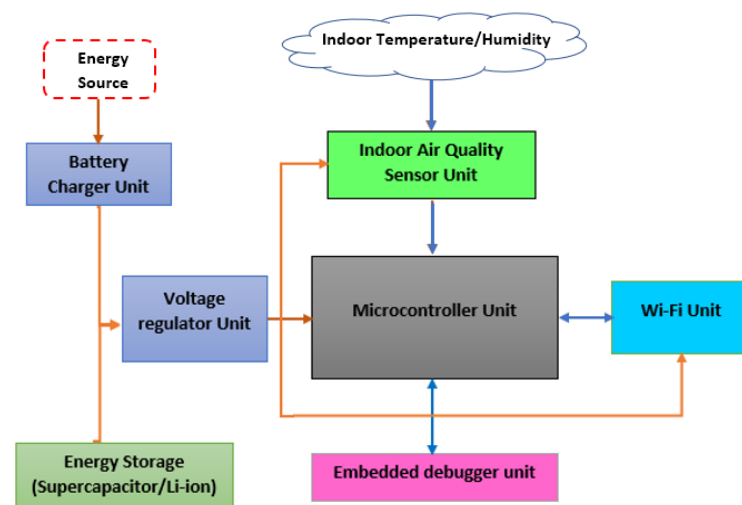
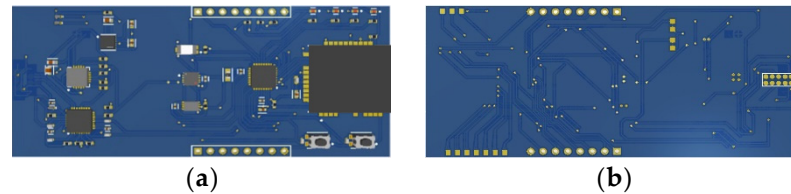**Figure 4.** Wireless climate sensor node architecture.

This study focused on low power consumption for autonomous operation and compact design aspects. The main power source node comes from either the supercapacitor or rechargeable Li-ion battery energy storage. The proposed node also has a battery charger unit for main power recharging purposes and future integration with an indoor energy harvesting system to fully work autonomously. The regulated voltage generated by the regulator unit supplies power to the main components, such as the IAQ sensor, microcontroller, and Wi-Fi transceiver. The acquired temperature and humidity data are transmitted and recorded to the IoT system through the Wi-Fi module for future indoor thermal comfort conditions assessment and analysis.

2.5.1. Hardware

The components were built into a single unit involving air quality sensor, microcontroller, Wi-Fi module, and power management that is also known as sensor node board. This integration follows the proposed block diagram as shown in Figure 4.

A.   Mainboard

The sensor node board design is shown in Figure 5. It was designed with a compact and small board based on the ATMEGA-4808 microcontroller.

(a)   (b)

Figure 5. PCB design of wireless climate sensor node: (**a**) top layer; (**b**) bottom layer.

The SMD components were applied on the sensor node to achieve low power consumption and compact board size. The node interfaced with a low-power temperature and humidity sensor using an I_2C interface to acquire temperature as well as relative humidity data and transmit to the cloud over a Wi-Fi module.

The sensor node operation voltage ranges are from 3.3 V to 5 V; therefore, the power source from either supercapacitor or rechargeable battery is sufficient to power it within hours up to days. Its specification is presented in Table 4.

Table 4. Sensor node specification.

Specification	Description	Remarks
Operating voltage	3.3–5 V	
Transceiver	Wi-Fi	2.412–2.472 MHz
Sensor interface	I_2C	
Sensing range	4 to 125 °C 0 to 100%	temperature range RH range
Power storage	Supercapacitor	
Size	25 mm × 60 mm	

The ATMega-4808 applied on the sensor node board is one of the AVR family microcontrollers with a low-power feature. Its specifications are presented in Table 5.

Table 5. ATMega-4808 specification. Adapted from ref. [29].

Specification	Description
Max ADC Resolution (bits)	10
CPU Speed (MIPS/DMIPS)	20
ADCs	1
Memory Size (KB)	48
Comparators	1
DigitalTimerQty_16 bit	4
Data EEPROM (bytes)	256
SPI	1
Mtrl Cntrl input capture	12
I_2C	1
Temp Range (°C)	−165
USART	3

Table 5. *Cont.*

Specification	Description
Voltage Operating	1.8–5.5
ADC Channels	12
Pin Count	32
Output comparator PWM	9
Program Memory Type	Flash
Ethernet	None
Low power	Yes

B.   Power storage

In general application, the battery and supercapacitor are most chosen as power storage because such devices are appealing with high storage efficiency. Both of them vary in cycle lifetime, charge and discharge times, as well as the complexity of changing circuits when implemented in the system. Their comparison is shown in Table 6.

Table 6. Power storage comparation. Adapted from ref. [30].

Parameters	Supercapacitor	Battery
Recharge Cycle Lifetime	$>10^6$ cycles	$<10^3$ cycles
Fastest discharging time	<a few min	0.3–3 h
Power Density (W/kg)	high (500–400)	low (50–300)
Voltage	0 V–2.7 V	3.7 V–4.2 V
The energy density (Wh/kg)	low (0.8–10)	high (20–150)
Self-discharge rate	30%	5%
Fastest charging time	s–min	hours
Changing circuit	simple	complex

According to Table 6, the supercapacitor units are more suitable as the power storage of the proposed sensor node. Since it has a higher power density and faster charge–discharge time, it can support a low-power sensor node system. In addition, it can be simply charged by using a battery charger unit. Two units of 5.5 V/5.0 F supercapacitor with a parallel connection provide more capacity; hence, the total value of 5.5 V/10 F was used as power storage. Figure 6 shows the supercapacitors after integrating into a parallel circuit.

Figure 6. Supercapacitor.

C.   Wi-Fi module

Microchip ATWINC1510 is an IoT network controller from the IEEE 802.11 b/g/n. The SPI-to-Wi-Fi interface has become the most used Wi-Fi and network add-on for existing

MCU solutions. The WINC1510 interfaces to any SAM or PIC MCU with minimum resource requirements. A single stream 1×1 802.11n is the WINC1510 most sophisticated mode. It has a built-in switch, power management, power amplifier, and LNA. Firmware can be stored in its internal Flash memory. Furthermore, it simply requires a high-speed crystal or oscillator as an external clock source (26 MHz). The WINC1510 is available in a QFN package or as a certified module. Figure 7 shows its embodiment that will later be integrated with a microcontroller unit. The detailed specification of WINC1510 is shown in Table 7.

Figure 7. Wi-Fi module WINC1510.

Table 7. Wi-Fi WINC1510 specification. Adapted from ref. [31].

Specification	Description
Type	Wi-Fi Module
Antenna	PCB, U.FL
Interface	SPI
External PA Control	No
Pin Count	28
Flash (KB)	4 Mb
Frequency	2.412–2.472 MHz
Temp Max.	+85 °C
Temp Min.	−40 °C
Volt Max.	4.2 V
Volt Min.	3.0 V
Power Output	18.5 dBm
Package	Surface Mount Module
Tx Current Cons.	287 mA
Rx Current Cons.	83 mA
Sleep Mode Current Cons.	4 μA
Input Sensitivity	−95

D.   Temperature and Humidity sensor

The SHT sensor module was applied to acquire temperature and relative humidity levels. The sensor contains an SHT3x-DIS IC chip from Sensirion with a high signal-to-noise ratio. It offers enhanced and reliable signal processing, fully calibrated with linearized digital output [32]. The best measurement results were obtained when the temperature range was approximately 5–60 °C (0.015 resolution), and the humidity range was between 20% and 80% RH (0.01 resolution). Figure 8 shows the SHT click sensor module, with comprehensive specifications listed in Table 8.

Figure 8. SHT click sensor module.

Table 8. SHT click sensor module specification. Adapted from ref. [32].

Specification	Description
Type	temperature and humidity
Input Volt	3.3 V–5 V
Module size	28.6 × 25.4 mm
Built-in modules	Sensiron's SHT3x-DIS IC
Compatibility	mikroBUS
Interface	GPIO, I_2C
Features	40 to 125 °C of temperature range. 0 to 100% of RH range ±2% RH and ±0.3 °C of accuracy
Applications	A precise, reliable, and quick measure of humidity and temperature

2.5.2. Software

The software of this system was developed using Arduino IDE as the base code environment and compiler. The code determines the flow of the logic step from the data sensing until the data from the sensor node are displayed. The program also defines a low-power operation; hence, the node can be less power-consuming, and meanwhile, the data were collected in a full cycle in seconds. In addition to low power, the reliable connection of the sensor node with the IoT interface in the cloud is also required to be set based on the ID and Key of the microcontroller board. The Adafruit Dashboard from adafruit.io was used to interface with the cloud and visualize the recorded temperature as well as the humidity data trend in a graphical user interface (GUI). The program's algorithm is described with the pseudo-code as follows (Algorithm 1).

Algorithm 1. The logical flow of smart wireless climate sensor node

---

Start program sensor node activity while power is ON.
Initialize wireless Internet connection.
If Wi-Fi is connected successfully:
    Start temperature and humidity level measurement,
    Process the data of temperature and humidity,
    Send measured data from the sensor to IoT cloud interface,
    Print data temperature and humidity to the IoT page,
    Wait to standby and set a low-power mode until a one-minute cycle is achieved.
Or else:
    Retry Wireless Connection Internet.
    Return to repeat measuring data.
Stop sensor node activity while power is OFF.

---

3. Result and Discussion

All sensor node main components were integrated and equipped with a supercapacitor on a 25 mm × 60 mm board of wireless climate sensor node. Several tests, validation, experiment, evaluation, and comprehensive analysis were conducted to ensure that the developed sensor node works properly according to design.

3.1. Device Implementation

The sensor node prototype is shown in Figure 9. As presented in the system architecture in Figure 4, all blocks were integrated to build the sensor node. It was implemented in a compact and small single board for easy installation (occupied small space) in indoor air quality monitoring applications and further development. The developed wireless climate sensor node will be integrated with indoor energy harvesting as a power source in further studies.

| (a) | (b) | (c) |
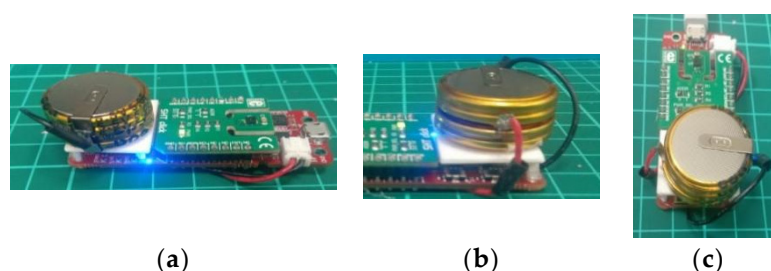
Figure 9. Wireless climate sensor node prototype: (**a**) side view; (**b**) energy source (supercapacitor); (**c**) top view.

3.2. Functionality Testing

Testing was conducted in every main block to ensure the device works properly. The testing was divided into three main blocks: power storage, processor, and wireless. The power storage was tested by connecting the sensor node with the power source for the supercapacitor charging process. The energy source used in this testing was a 5 V external power supply connected to the sensor node with a micro cable connector. Meanwhile, the discharging process was carried out by removing the sensor node from the external power supply. The system will switch to the supercapacitor as the power source. The processor unit was tested by programming the system to communicate with the sensor and read the temperature and humidity parameters. The reading is very fundamental because both parameters will be processed to analyze the thermal comfort value. Further testing was conducted on the wireless unit. This is inseparable from the processor test in the previous block because it involves the programming process. The unit can maintain a Wi-Fi connection and send data to the server that indicate that the wireless function is running well. All results are presented in Table 9.

Table 9. Functionality testing results.

Block	Testing Parameter	Result
Power storage	Charging and discharging supercapacitor	Work properly
Processor	Sensor measurement and scanning Wi-Fi availability	Work properly
Wireless	Connection and transmitting ability	Work properly

3.3. Calibration

The developed sensor node produces two data parameters, temperature and humidity, which are used to determine the thermal comfort level in a room. Calibration was carried out to ensure that the value generated by the sensor node is the same as other standardized measuring instruments. During this process, the Graphtec temperature and humidity

(GS-TH) probe was connected to the GL840 data logger as shown in Figure 10a, which can measure temperature between −20–85 °C and humidity in the range of 0–100%. Calibration was carried out through three stages: measurement, calibration compensation calculation, and validation.

(**a**)   (**b**)

Figure 10. Calibration process of wireless climate sensor node: (**a**) measurement setup, (**b**) sensor node placement in a controllable test chamber.

3.3.1. Measurement

The measurement process was conducted by placing the sensor node and Graphtec GS-TH probe on a controllable test chamber, as shown in Figure 10b. This chamber was used because it can generate heat up to 60 °C. Table 10 shows the comparison of temperature and humidity measurements results between the sensor node and the Graphtec GS-TH probe. The temperature and humidity average error is 5.24 °C and −8.82%, respectively.

Table 10. Measurement results before calibration.

Sensor Node		Validator		Difference	
Temperature (°C)	Humidity (%)	Temperature (°C)	Humidity (%)	Temperature (°C)	Humidity (%)
30.00	45.45	25.02	55.30	4.98	−9.85
30.76	44.13	25.53	53.90	5.23	−9.77
31.38	42.98	26.04	52.50	5.34	−9.52
31.93	42.08	26.56	51.50	5.37	−9.42
32.42	40.95	27.02	50.50	5.40	−9.55
32.87	40.14	27.53	49.30	5.34	−9.16
33.25	39.44	28.00	48.20	5.25	−8.76
33.54	38.72	28.51	46.60	5.03	−7.88
34.24	38.02	29.03	46.00	5.21	−7.98
34.78	37.23	29.54	44.90	5.24	−7.67
35.21	36.39	30.00	43.80	5.21	−7.41
Error Average				5.24	−8.82

3.3.2. Calibration Compensation Calculation

All temperature and humidity measurement data were used to determine the calibration compensation factor value at the measurement stage. Figures 11 and 12 are the results of processing temperature and humidity data using Microsoft Excel software. Calibration compensation for temperature is $y = 0.9938x - 5.0317$ and humidity is $y = 1.293x - 3.0518$. Both values will be used in the program to compensate for each sensor measurement result.

3.3.3. Validation

The latest program was included with a calibration compensation factor for each parameter and used for re-measurement with the same procedure as the measurement stage. Measurements at this stage were carried out to validate the results of temperature

and humidity readings after being calibrated. Table 11 shows the average error for each parameter decreased to around zero, where the temperature was −0.05 °C, and humidity was 0.08%. This value indicated that the developed sensor node provides measurement data results close to the value of the standardized measuring instruments.
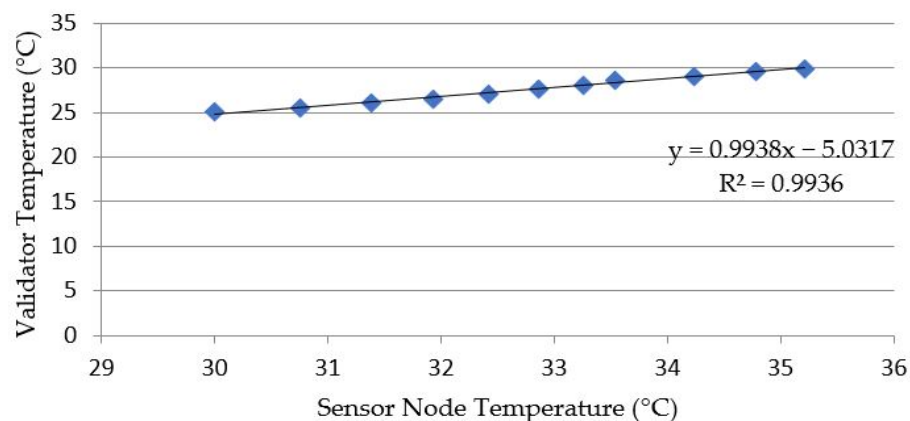

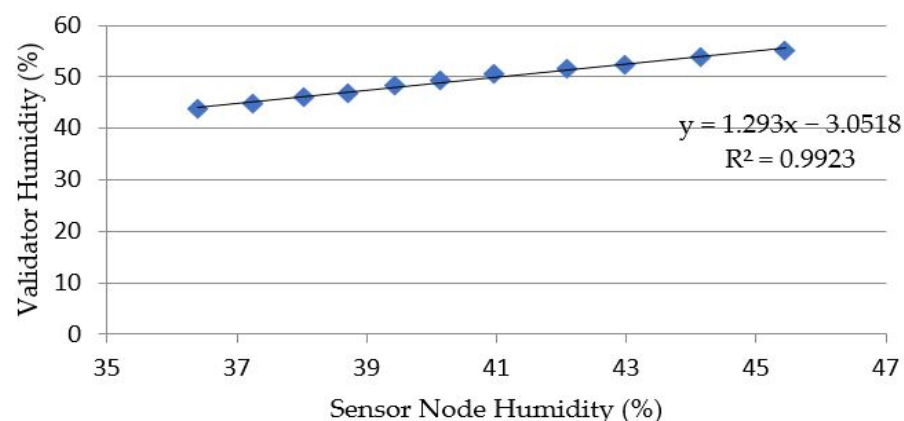**Figure 11.** Temperature compensation calculation.

Figure 12. Relative humidity calculation.

Table 11. Temperature and humidity results after calibration.

Sensor Node		Validator		Difference	
Temperature (°C)	Humidity (%)	Temperature (°C)	Humidity (%)	Temperature (°C)	Humidity (%)
25.93	56.64	26.04	56.30	−0.11	0.34
26.36	55.07	26.52	54.80	−0.16	0.27
27.05	53.59	27.02	53.40	0.03	0.19
27.68	51.81	27.66	52.40	0.02	−0.59
28.02	50.93	28.04	51.40	−0.02	−0.47
28.47	49.93	28.55	50.40	−0.08	−0.47
28.73	48.88	29.03	48.20	−0.30	0.68
29.49	46.92	29.50	46.60	−0.01	0.32
30.02	45.79	30.00	45.50	0.02	0.29
30.61	44.86	30.56	44.70	0.05	0.16
30.97	43.79	30.98	43.6	−0.01	0.19
	Error Average			−0.05	0.08

3.4. Power Capacity Requirement

The developed climate sensor node was programmed with a low-power mode algorithm to work with low power consumption. The measurement of power consumption is presented in this section by dividing the section into three stages: current measurement, time consumption measurement, and power consumption measurement. One working cycle of this device is divided into six processes, and the function of each is described in Table 12.

Table 12. Wireless climate sensor node working processes.

Process	Description
Initializing	All variable preparation and disable low-power mode
SHT Sensor Reading	SHT working to measure temperature and humidity
Temperature data transmitting	Transmit temperature data to the server
Humidity data transmitting	Transmit humidity data to the server
Log data transmitting	Transmit temperature and humidity data to the server
Low-power mode	Enable low-power mode

3.4.1. Current Measurement

The current measurement in this stage utilized a 1NA219 sensor. The sensor was assembled and programmed with Arduino Mega. The Arduino board and 1NA219 sensor node used a different power source from the sensor node to ensure no interference with the measurement results. Figure 13 shows the circuit used during the measurement.
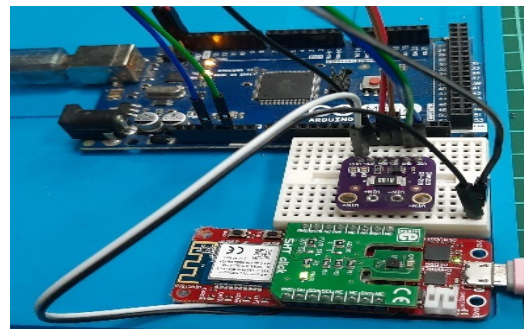
Figure 13. Current measurement process.

Figure 14 shows the current measurement of each process. The initializing and SHT sensor reading were 28.90 mA and 101.40 mA, respectively, while transmitting approximately had 114 mA for each dataset, and 29.03 mA when the low-power mode was enabled.
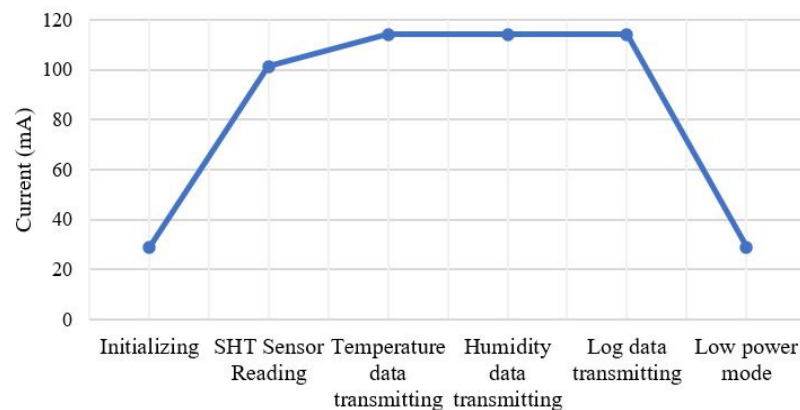
Figure 14. Current measurement result for one working cycle.

3.4.2. Time Consumption

Time consumption is a measurement of time carried out on each process in one working cycle of the developed sensor node. This test was conducted to analyze the estimation of the system power requirement. The whole process was measured using programming techniques to determine the time consumption in each process. However, in the last process, the low-power mode was similar to the time interval set in the program. During this interval, the developed sensor node enables the low-power mode and when the interval is reached, it returns to work in the initializing process by disabling the low-power mode. This technique is used to reduce power consumption. This means that the developed sensor node will only work for initializing, sensor reading, and transmitting data at certain time intervals. There are two reasons underlying the use of the interval technique. First, the power required when the low-power mode is enabled is much less than when it is disabled. Second, the changes in temperature and humidity in the room are not significant in a short time. The timing of the 10 s interval is to reduce power consumption but still provide real-time temperature and humidity data. The time required for the initializing process was approximately 662 ms and the SHT sensor reading process took 23.8 ms. Meanwhile, data transmitting for temperature, humidity, and log took 1461.2 ms, 1365.2 ms, and 1134.2 ms, respectively. All the data were obtained from the five measurement times of processing time consumption, as shown in Figure 15.
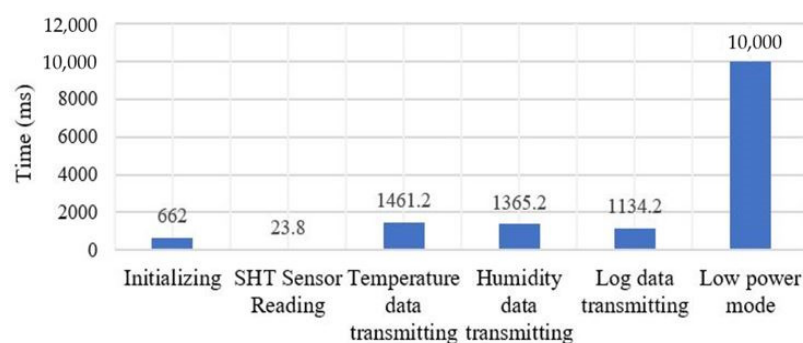

Figure 15. Time consumption.

3.4.3. The Energy Capacity

The energy capacity required can be calculated based on power calculation and time consumption data. Table 13 shows the developed sensor node power calculation required in one cycle with the interval set to 10 s. The biggest power consumption was at the temperature data transmitting process of 372.93 mW. However, the biggest energy capacity required was in the low-power mode process of 0.263 mWh. This was due to the time interval that was set at 10 s. The total energy capacity required in one cycle of the node measuring the data was 0.693 mWh. Figure 16 shows the percentage of each process in the energy capacity requirement.

Table 13. Energy capacity.

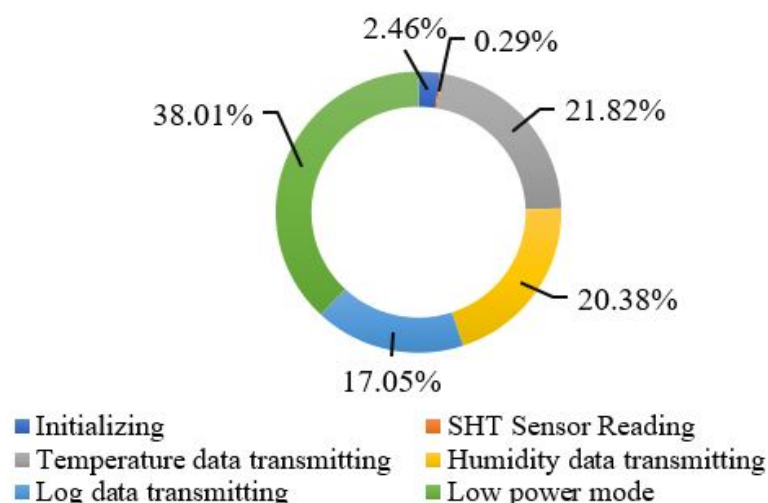| Process	Voltage (V)	Current (mA)	Power (mW)	Time (ms)	Energy Capacity Required (mWh)
Initializing		28.90	94.23	662.00	0.017
SHT Sensor Reading		101.40	331.3	23.80	0.002
Temperature data transmitting	3.3	114.13	372.93	1461.20	0.151
Humidity data transmitting		114.07	372.93	1365.20	0.141
Log data transmitting		114.27	373.39	1134.20	0.118
Low-power mode		29.03	94.65	.00	0.263
					0.693

Figure 16. Energy capacity requirement percentage.

3.4.4. Power Storage Testing

Storage testing was carried out by charging and discharging the supercapacitor. The sensor node was equipped with a supercapacitor of 10 F/5.5 V capacity. The required energy capacity in one work cycle of the sensor node is 0.693 mWh. In this experiment, testing was conducted to measure how long the supercapacitor needs the charging and discharging time. The charging process was carried out by connecting the sensor node with a 5 V external power supply over a USB to a micro-USB connector. Meanwhile, discharging was conducted by removing the connector from the external power source. The supercapacitor will function as a power source for the sensor node. Figure 17 shows the results of measuring the charging and discharging time. The charging process took 170 s to increase the voltage from 3.0 V to 4.3 V, while the discharging can drive the sensor node for 180 s. These results indicated a good start in using supercapacitors as power storage. In the future, they will be connected to an indoor energy source that utilizes energy harvesting from indoors.
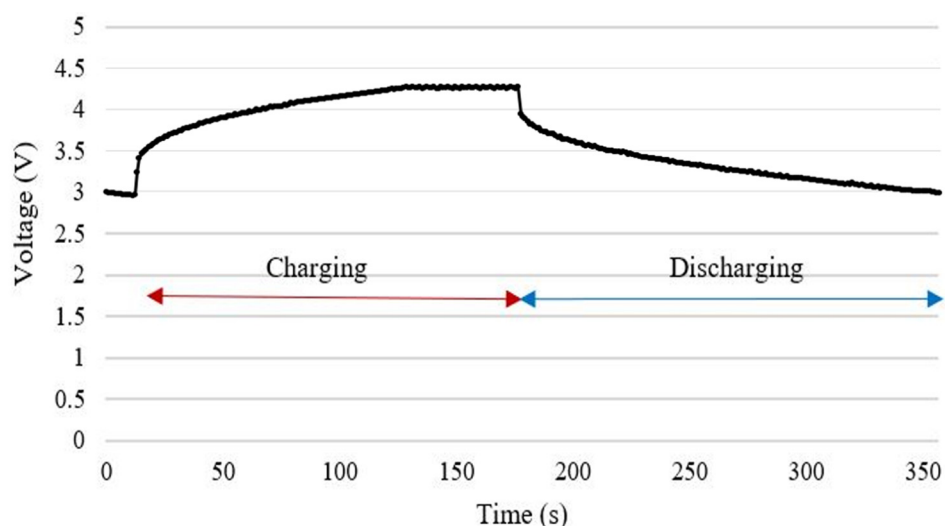
Figure 17. Charging and discharging process.

3.5. User Interface

This dashboard was created using the Adafruit platform to visualize the temperature and relative humidity data trends. A temperature and humidity meter panel shows the last values of these parameters measured by the wireless climate sensor node. In addition, there is a temperature and humidity history data graph that can display data in the last

few days. The chart is equipped with a data log that contains time information and all data received by the dashboard. The monitoring dashboard can also generate alert notifications when the temperature and relative humidity are over the thermal comfort threshold level. Figure 18 shows a dashboard that was created and can display both parameters' data.
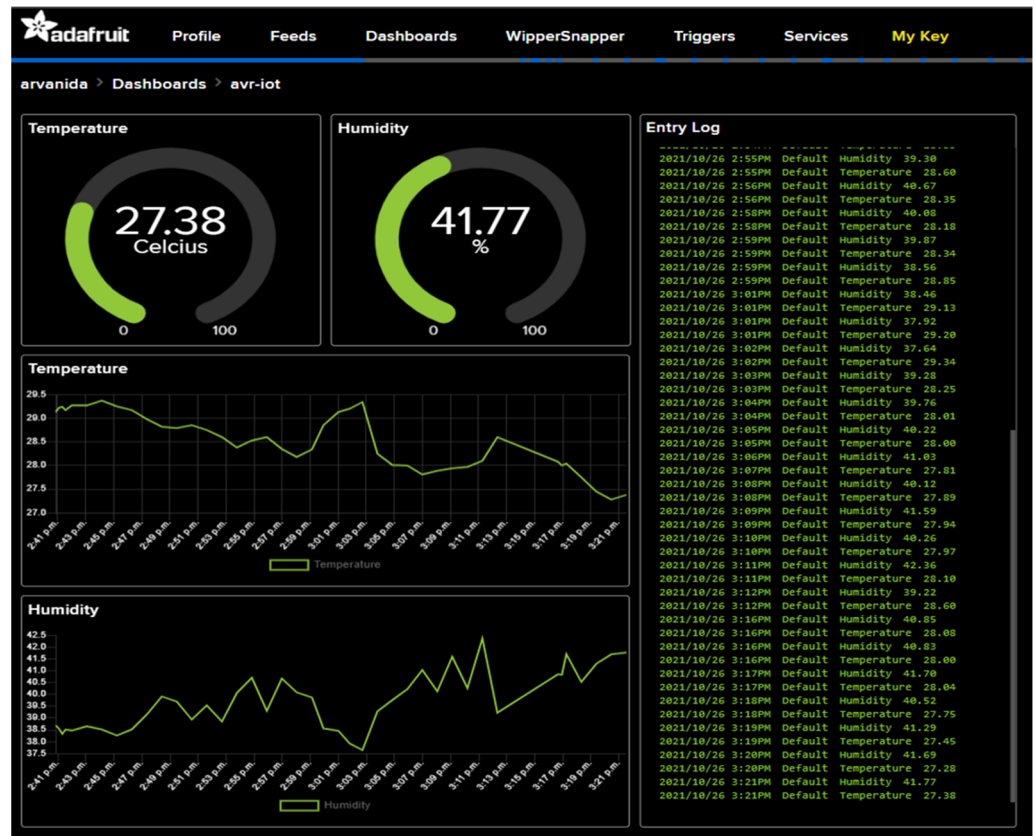

Figure 18. Dashboard monitoring.

3.6. Thermal Comfort Measurement Experiment

3.6.1. Configuration

The sensor node read the room temperature and humidity parameters and sent the data to the IoT core. The data received by the core were displayed in the monitoring dashboard and used for further analysis. Figure 19 shows the configuration used in this experiment.
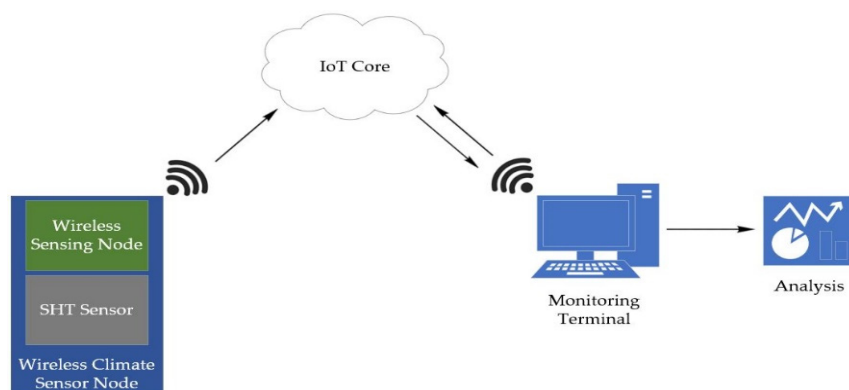
Figure 19. Wireless climate sensor node testing setup.

3.6.2. Result

During 4 days of testing from 10 to 13 January 2022, the sensor node worked by sending data to the IoT core. Figures 20 and 21 show temperature and humidity data graphs during the field experiment.
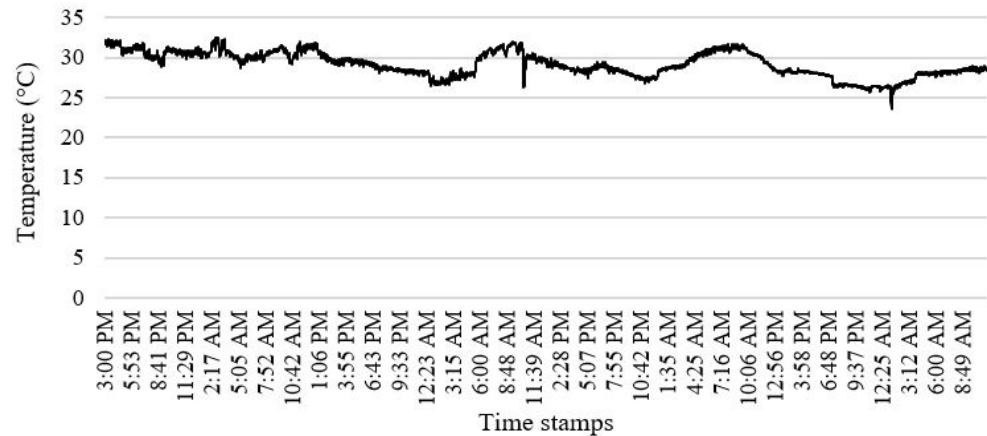

Figure 20. The recorded temperature data trends.

Figure 21. The recorded Relative Humidity data trends.

4. Conclusions

A smart wireless climate sensor node prototype for indoor temperature and relative humidity monitoring application was implemented in this study. With a compact size in a single board which only consumes a total energy capacity required of 0.693 mWh per cycle of data measurement (initialization, data acquired, data transmitted, and power mode) in 14.65 s, the device is suitable for low-power and long-term indoor thermal comfort assessment purposes. Moreover, the highest energy required is 0.26 mWh, which is 38.01% of the node's total consumption observed during the low-power mode with a time interval 10 s. The results of measurement performance indicated that the device had an accuracy of −0.05 °C and 0.08% for temperature and RH measurement, respectively. In addition, it was able to monitor indoor thermal comfort in a temperature average of 25–30 °C and humidity average of 30–40% during a 4 day field experiment. The acquired data were successfully transmitted to the cloud over the IoT system, while the trends were displayed and recorded in the monitoring terminal dashboard for further analysis. From the power requirement perspective, the 10 F supercapacitor can provide energy to the sensor node for 180 s. However, the power storage can still extend its lifetime by either increasing the storage capacity or harvesting energy from the indoor environment. Therefore, with a low power consumption feature, the developed wireless climate sensor node has the potential

to integrate with an indoor energy harvesting system (micro-scale energy) toward a fully autonomous active sensor node for a long operating time.

References

1. Krzaczek, M.; Tejchm, J. Indoor Air Quality and Thermal Comfort in Naturally Ventilated Low-Energy Residential Houses. In *Air Quality—Monitoring and Modeling*; Kumar, S., Ed.; InTech Open: London, UK, 2012. [CrossRef]
2. Zeiler, W.; Houten, R.V.; Boxem, G.; Vissers, D.; Maaijen, R. Indoor Air Quality and Thermal Comfort Strategies: The Human-Inthe-Loop Approach. 2011. Available online: https://www.semanticscholar.org/paper/Indoor-Air-Quality-And-Thermal-Comfort-Strategies-%3A-Zeiler-Houten/3a08f049c9dc4d2e1614d83bb130cc7fa6e2ddf2 (accessed on 15 February 2022).
3. Nilsson, H.O.; Holmér, I. Comfort climate evaluation with thermal manikin methods and computer simulation models: Comfort climate evaluation. *Indoor Air* **2003**, *13*, 28–37. [CrossRef]
4. Ahmed, M.S.; Mohamed, A.; Homod, R.Z.; Shareef, H.; Khalid, K. Awareness on Energy Management in Residential Buildings: A Case Study in Kajang and Putrajaya. Undefined. 2017. Available online: https://www.semanticscholar.org/paper/Awareness-on-energy-management-in-residential-A-in-Ahmed-Mohamed/519d0a685e12ff7917d534ff52eacd11c3cfed74 (accessed on 15 February 2022).
5. Engelmann, P.; Roth, K.; Tiefenbeck, V. *Comfort, Indoor Air Quality, and Energy Consumption in Low Energy Homes*; U.S. Department of Energy, Energy Efficiency & Renewable Energy: Washington, DC, USA, 2013.
6. Pereira, L.D.; Raimondo, D.; Corgnati, S.P.; da Silva, M.G. Assessment of indoor air quality and thermal comfort in Portuguese secondary classrooms: Methodology and results. *Build. Environ.* **2014**, *81*, 69–80. [CrossRef]
7. Szczepanik-Ścisło, N.; Flaga-Maryańczyk, A. Measurements and simulation of CO_2 concentration in a bedroom of a passive house. *Cazsopismo Tech.* **2018**, *9*, 163–180. [CrossRef]
8. Berardi, U.; Manca, M. The Energy Saving and Indoor Comfort Improvements with Latent Thermal Energy Storage in Building Retrofits in Canada. *Energy Procedia* **2017**, *111*, 462–471. [CrossRef]
9. Silveira, E.; Bonho, S. Temperature Monitoring Through Wireless Sensor Network Using an 802.15.4/802.11 Gateway. *IFAC Pap. Online* **2016**, *49*, 120–125. [CrossRef]
10. Kumar, A.; Hancke, G.P. An Energy-Efficient Smart Comfort Sensing System Based on the IEEE 1451 Standard for Green Buildings. *IEEE Sens. J.* **2014**, *14*, 4245–4252. [CrossRef]
11. Adiono, T.; Fathany, M.Y.; Fuada, S.; Purwanda, I.G.; Anindya, S.F. A portable node of humidity and temperature sensor for indoor environment monitoring. In Proceedings of the 2018 3rd International Conference on Intelligent Green Building and Smart Grid (IGBSG), Yi-Lan, Taiwan, 22–25 April 2018; pp. 1–5. [CrossRef]
12. Indoor Air Quality: Indoor Comfort Quality. Available online: http://www.healthyheating.com/Thermal_Comfort_Working_Copy/IAQ_ICQ_IEQ.htm (accessed on 27 November 2021).
13. Darji, C.P. IoT Based Sensor for Humidity and Temperature Measurement in Smart HVAC Systems. *IJRTE* **2021**, *9*, 42–44. [CrossRef]
14. Scislo, L.; Szczepanik-Scislo, N. Air quality sensor data collection and analytics with iot for an apartment with mechanical ventilation. In Proceedings of the 2021 11th IEEE International Conference on Intelligent Data Acquisition and Advanced Computing Systems: Technology and Applications (IDAACS), Cracow, Poland, 22–25 September 2021; pp. 932–936. [CrossRef]
15. Al Horr, Y.; Arif, M.; Katafygiotou, M.; Mazroei, A.; Kaushik, A.; Elsarrag, E. Impact of indoor environmental quality on occupant well-being and comfort: A review of the literature. *Int. J. Sustain. Built Environ.* **2016**, *5*, 1–11. [CrossRef]

16. Elforjani, B.; Feng, G.; Gu, F.; Ball, A.D. Thermal Energy Harvesting in Wireless Temperature Sensor Nodes for Condition Monitoring. *Int. J. COMADEM* **2021**, *20*. Available online: https://apscience.org/comadem/index.php/comadem/article/view/28 (accessed on 11 December 2021).

17. Wu, X.; Liu, Y.; Liu, G.; Wang, F.; Wang, Z. Effect of Supply Air Temperature on Indoor Thermal Comfort in a Room with Radiant Heating and Mechanical Ventilation. *Energy Procedia* **2017**, *121*, 206–213. [CrossRef]

18. Evaluation of Human Thermal Comfort Using by Meteorological Approach (2008—13MontMet17AP_17appclim). Available online: https://ams.confex.com/ams/13MontMet17AP/techprogram/paper_141147.htm (accessed on 15 February 2022).

19. Wu, J. Thermal Comfort and Occupant Behaviour in Office Buildings in South-East China. 16 July 2015. Available online: http://eprints.nottingham.ac.uk/29435/ (accessed on 15 December 2021).

20. Wang, X.; Yang, L.; Gao, S.; Zhao, S.; Zhai, Y. Thermal comfort in naturally ventilated university classrooms: A seasonal field study in Xi'an, China. *Energy Build.* **2021**, *247*, 111126. [CrossRef]

21. How Smart Climate Control Benefits Employee Wellness. Available online: https://www.triplepundit.com/story/2013/how-smart-climate-control-benefits-employee-wellness/53346 (accessed on 18 December 2021).

22. Alhefnawi, M.A.M. Thermal Comfort and Gender A Practical Study in the Eastern Province of Saudi Arabia. In Proceedings of the Eco house Initiative and Network for Comfort and Energy Use in Buildings, August 2020.

23. Peng, J.; Li, L.; Liu, F.; Chen, S. Application on Evaporative Cool Technique in Garment Workshop in Hot-Humid Area. *Procedia Engineering* **2015**, *121*, 2029–2036. [CrossRef]

24. Ali, B.A.; Ahmed, H.O.; Ballal, S.G.; Albar, A.A. Pulmonary Function of Workers Exposed to Ammonia: A Study in the Eastern Province of Saudi Arabia. *International Journal of Occupational and Environmental Health* **2001**, *7*, 19–22. [CrossRef]

25. Falke, R. "Doc" How Humidity Affects Comfort. Available online: https://www.contractingbusiness.com/service/article/20871274/how-humidity-affects-comfort (accessed on 15 February 2022).

26. Alsmo, T.; Alsmo, C. Ventilation and Relative Humidity in Swedish Buildings. *JEP* **2014**, *05*, 1022–1036. [CrossRef]

27. Federal-Provincial Advisory Committee on Environmental and Occupational Health (Canada) (Ed.) *Exposure Guidelines for Residential Indoor Air Quality: A Report of the Federal-Provincial Advisory Committee on Environmental and Occupational Health*; Health and Welfare Canada: Ottawa, ON, Canada, 1989.

28. Benammar, M.; Abdaoui, A.; Ahmad, S.; Touati, F.; Kadri, A. A Modular IoT Platform for Real-Time Indoor Air Quality Monitoring. *Sensors* **2018**, *18*, 581. [CrossRef] [PubMed]

29. ATMEGA 4808. Available online: https://www.microchip.com/en-us/product/ATMEGA4808 (accessed on 25 December 2021).

30. Kim, S.; Chou, P.H. Energy Harvesting with Supercapacitor-Based Energy Storage. In *Smart Sensors and Systems*; Lin, Y.-L., Kyung, C.-M., Yasuura, H., Liu, Y., Eds.; Springer International Publishing: Cham, Switzerland, 2015; pp. 215–241. ISBN 9783319147116.

31. ATWINC1510. Available online: https://www.microchip.com/en-us/product/ATWINC1500 (accessed on 25 December 2021).

32. SHT Click | Add-On Board with SHT3x Humidity and Temperature Sensor. MikroElektronika. Available online: http://www.mikroe.com/sht-click (accessed on 25 December 2021).